

Sub-Nyquist Radar via Doppler Focusing

Omer Bar-Ilan and Yonina C. Eldar, *Senior Member, IEEE*

Abstract—We investigate the problem of a monostatic radar transceiver trying to detect targets, sparsely populated in the radar’s unambiguous time-frequency region. Several past works employ compressed sensing (CS) algorithms to this type of problem, but either do not address sample rate reduction, impose constraints on the radar transmitter, or propose CS recovery methods with prohibitive dictionary size. Here, using the Xampling framework, we describe a sub-Nyquist sampling approach which has several important advantages over previous methods: low rate sampling and digital processing, undersampling in both fast and slow time, the resulting CS dictionary size is proportional to delay grid size only, and we impose no restrictions on the transmitter. Xampling allows reducing the number of samples needed to accurately represent the signal, directly in the analog-to-digital conversion process. Furthermore, our approach can be implemented in hardware using a previously suggested Xampling prototype. After sampling, the entire digital recovery process is performed on the low rate samples without having to return to the Nyquist rate. In the noiseless case, we can recover a sparse target scene from samples taken at a rate proportional to the signal’s rate of innovation, which can be several orders of magnitude smaller than its Nyquist rate. In the presence of noise, we introduce the concept of Doppler focusing from the low rate samples in order to obtain good detection performance even at SNRs as low as -25dB.

Index Terms—compressed sensing, rate of innovation, radar, sparse recovery, sub-Nyquist sampling, delay-Doppler estimation.

I. INTRODUCTION

We consider target detection and feature extraction in a radar system, using sub-Nyquist sampling rates. The radar is a single transceiver, monostatic, narrow-band pulse-train system. Targets are non-fluctuating point targets, sparsely populated in the radar’s unambiguous time-frequency region: delays up to the Pulse Repetition Interval (PRI), and Doppler frequencies up to its reciprocal the Pulse Repetition Frequency (PRF). We propose a recovery method which can detect and estimate targets’ time delay and Doppler frequency, using a linear, non-adaptive sampling technique at a rate significantly lower than the radar signal’s Nyquist frequency, assuming the number of targets L is small.

Current state-of-the-art radar systems sample at the signal’s Nyquist rate, which can be hundreds of MHz and even up to several GHz. Systems exploiting sub-Nyquist sampling rates can benefit from a lower rate analog-to-digital conversion (ADC), which requires less computational power. Moreover, sampling at the Nyquist rate may not always be feasible due to high power consumption, heat dissipation, cost, or other practical considerations. Finally, offline radar systems which

record samples for subsequent processing will gain substantial storage capacity reduction if they are able to sample at sub-Nyquist rates.

The goal of this work is to break the link between radar signal bandwidth and sampling rate. The sub-Nyquist Xampling (“compressed sampling”) [1] method we use is an ADC which performs analog prefiltering of the signal before taking point-wise samples. These compressed samples (“Xamples”) contain the information needed to recover the desired signal parameters using compressed sensing (CS) algorithms. This work expands the work in [2], adding Doppler to the target model and proposing a new method to estimate it. The same sampling technique and hardware that were used in [2], [3] will also work here, while the digital processing we suggest is different.

Past works employ compressed sensing (CS) algorithms to this type of problem, but do not address sample rate reduction and continue sampling at the Nyquist rate [4], [5]. Other works combine radar and CS in order to reduce the receiver’s sampling rate, but in doing so impose constraints on the radar transmitter and do not treat noise [6], or require an infinite number of samples [7]. Another line of work proposes single stage CS recovery methods with dictionary size proportional to the product of delay and Doppler grid sizes, making them infeasible for many realistic scenarios [5], [8].

Our approach is based on the observation that the received radar signal can be modeled with $3L$ degrees of freedom (DOF): a delay, Doppler frequency and amplitude for each of the L targets. Signals which can be described with a fixed number of DOF per unit of time are known as Finite Rate of Innovation (FRI) [9] signals. The proposed recovery process is actually a recovery of these DOF from low rate samples. The concept of FRI together with the Xampling methodology enables sub-Nyquist rates using practical hardware [1].

At the crux of our proposed method is a coherent superposition of time shifted and modulated pulses, the Doppler focusing function $\Phi(t; \nu)$. For any Doppler frequency ν , this function combines the received signals from different pulses so targets with appropriate Doppler frequencies come together in phase. For each sought after ν , $\Phi(t; \nu)$ is processed as a simple one-dimensional CS problem and the appropriate time delays are recovered. The gain from this method is both in terms of signal-to-noise ratio (SNR) and Doppler resolution. For P pulses adding coherently, we obtain a factor P SNR improvement over white noise (which adds incoherently, i.e. in power). In addition, denoting the PRI as τ , the width of the Doppler focus for each $\Phi(t; \nu)$ is $2\pi/P\tau$, meaning that delays of targets separated in Doppler by more than $2\pi/P\tau$ will not interfere with each other.

The idea for Doppler focusing comes from a similar function in the context of ultrasound beamforming used in [10].

The authors are with the Department of Electrical Engineering, Technion–Israel Institute of Technology, Haifa, Israel 32000 (phone: +972-4-8294798, +972-4-8294682, fax: +972-4-8295757, e-mail: omerba@tx.technion.ac.il, yonina@ee.technion.ac.il).

There, in a method named “Dynamic focusing”, the signal returned to a set of linearly aligned transceivers is focused in a manner similar to how we focus pulses, and the Doppler frequency ν is replaced by spatial direction θ . In both cases, the advantages of focusing are not lost with sub-Nyquist processing since it can be performed on the low rate Xamples and improves the SNR.

Simulations provided in Section VII show that when sampling at one tenth the Nyquist rate, our Doppler focusing recovery method outperforms both two-stage CS recovery and classic processing. When the SNR reaches -25dB, our approach achieves the performance of classic matched filtering (MF) operating at the full Nyquist rate.

The main merits of our proposed method are as follows:

- 1) **Low rate ADC and DSP** – using Xampling and the proposed recovery method, we are able to acquire the sub-Nyquist samples containing information needed for target recovery, and then digitally recover the unknown target parameters using low rate processing, without returning to the higher Nyquist rate.
- 2) **Undersampling in both fast and slow time** – our method allows for sample rate reduction both in the intra-pulse (“fast time”) and the inter-pulse (“slow time”) samples. This provides an additional degree of freedom in the algorithm, facilitating improved design of system architecture and hardware. For example, systems with a constraint on average (as opposed to instantaneous) sample rate may choose to alleviate the fast time sample rate reduction at the expense of reducing slow time sample rate.
- 3) **Scaling with problem size** – many CS delay-Doppler estimation methods depend upon constructing a CS dictionary with a row for each delay-Doppler hypothesis. For even moderate size problems, the number of delay or Doppler hypotheses (i.e. grid sizes) can easily be on the order of 10^3 , with a number of measurements of similar order. This entails the dictionary to possess 10^9 elements, which is infeasible for many systems, especially real-time ones. Our Doppler focusing based method avoids this problem by separating the Doppler from delay recovery, making each CS delay recovery indifferent to the underlying Doppler.
- 4) **Transmitter compatibility** – our recovery method does not impose any restrictions on the transmitted signal, provided it meets the assumptions stated in Section II.

The remainder of this paper is organized as follows. In Section II we describe the radar model and the assumptions used for simplification. Section III reviews classic matched filter processing. We explain the Doppler focusing concept in Section IV and sub-Nyquist delay recovery in Section V. The delay-Doppler recovery method using Doppler focusing is described in Section VI, and numerical results are presented in Section VII.

We denote vectors by boldface lower case letters, e.g. \mathbf{c} , and matrices by boldface capital letters, e.g. \mathbf{A} . We say a vector \mathbf{c} is L -sparse if $\|\mathbf{c}\|_0 \leq L$, i.e. at most L of its elements are nonzero. The n th element of a vector is written as c_n , and the ij th element of a matrix is denoted by \mathbf{A}_{ij} .

Non-boldface variables represent scalars or functions, where continuous functions are denoted with round parentheses, e.g. $x(t)$ and discrete functions with square parentheses, e.g. $h[n]$.

II. RADAR MODEL

We consider a radar transceiver that transmits a pulse train

$$x_T(t) = \sum_{p=0}^{P-1} h(t - p\tau), \quad 0 \leq t \leq P\tau \quad (1)$$

consisting of P equally spaced pulses $h(t)$. The pulse-to-pulse delay τ is referred to as the PRI, and its reciprocal $1/\tau$ is the PRF. The pulse $h(t)$ is a known time-limited baseband function with continuous-time Fourier transform (CTFT) $H(\omega) = \int_{-\infty}^{\infty} h(t)e^{-j\omega t} dt$. We assume that $H(\omega)$ has negligible energy at frequencies beyond $B_h/2$ and we refer to B_h as the bandwidth of $h(t)$. The target scene is composed of L non-fluctuating point targets (Swering 0 model, see [11]), where we assume that L is known, although this assumption can easily be relaxed. The pulses reflect off the L targets and propagate back to the transceiver. Each target l is defined by three parameters: a time delay τ_l , proportional to the target’s distance from the radar; a Doppler radial frequency ν_l , proportional to the target-radar closing velocity; and a complex amplitude $\alpha_l \in \mathbb{C}$, proportional to the target’s radar cross section (RCS), dispersion attenuation and all other propagation factors. We limit ourselves to defining targets in the radar’s radial coordinate system; future work will deal with targets’ angular properties.

Throughout, we make the following assumptions on the targets’ location and motion, which allow us to obtain a simplified expression for the received signal. See the Appendix for details.

- A1.** “Far targets” - target-radar distance is large compared to the distance change during observation interval which allows for constant α_l .
- A2.** “Slow targets” - small target velocity allows for constant τ_l during observation interval and constant Doppler phase during pulse time T_p .
- A3.** “Small acceleration” - target velocity remains approximately constant during observation interval allowing for constant ν_l .

Although these assumptions may seem hard to comply with, they all rely on slow “enough” relative motion between the radar and its targets. Radar systems tracking people, ground vehicles and sea vessels usually comply quite easily. For example, consider a $P=100$ pulse radar system with PRI $\tau=100\mu\text{sec}$, pulse width $T_p=1\mu\text{sec}$, bandwidth $B_h=30\text{MHz}$ and carrier frequency $f_c=3\text{GHz}$, tracking cars traveling up to 120km/hour. The maximal distance change over observation interval is approximately 0.33m, so if the targets’ minimal distance from the radar is a few meters, then **A1.** is satisfied. As for **A2.**, the maximal Doppler frequency is approximately 667Hz, which is much smaller than both $f_c/P\tau B_h=10\text{KHz}$ and $1/T_p=1\text{MHz}$. An extreme acceleration of 10m/sec^2 would cause a velocity change of 0.1m/sec over observation interval, easily satisfying **A3.** As for airborne targets, care must be taken to ensure compliance.

Using these three assumptions, we can write the received signal as

$$x(t) = \sum_{p=0}^{P-1} \sum_{l=0}^{L-1} \alpha_l h(t - \tau_l - p\tau) e^{-j\nu_l p\tau}. \quad (2)$$

It will be convenient to express the signal as a sum of single frames

$$x(t) = \sum_{p=0}^{P-1} x_p(t) \quad (3)$$

where

$$x_p(t) = \sum_{l=0}^{L-1} \alpha_l h(t - \tau_l - p\tau) e^{-j\nu_l p\tau}. \quad (4)$$

In reality $x(t)$ will be contaminated by additive noise. We will take this into account in our simulations.

Since the transmitted signal (1) is a finite periodic pulse train, it is invariant to the transformation $\tau_l \rightarrow \tau_l + k_1\tau$, $\nu_l \rightarrow \nu_l + 2\pi k_2/\tau$ where $k_1, k_2 \in \mathbb{Z}$, except on its boundaries. Specifically, assuming that $k_1 \ll P$,

$$\begin{aligned} & \sum_{p=0}^{P-1} \sum_{l=0}^{L-1} \alpha_l h(t - (\tau_l + k_1\tau) - p\tau) e^{-j(\nu_l + 2\pi k_2/\tau)p\tau} \\ &= \sum_{p=k_1}^{P-1+k_1} \sum_{l=0}^{L-1} \alpha_l h(t - \tau_l - p\tau) e^{-j\nu_l(p-k_1)\tau} \\ &= \sum_{p=k_1}^{P-1+k_1} \sum_{l=0}^{L-1} \alpha_l e^{j\nu_l k_1\tau} h(t - \tau_l - p\tau) e^{-j\nu_l p\tau} \\ &= \sum_{p=k_1}^{P-1+k_1} \sum_{l=0}^{L-1} \tilde{\alpha}_l h(t - \tau_l - p\tau) e^{-j\nu_l p\tau}, \end{aligned} \quad (5)$$

with $\tilde{\alpha}_l = \alpha_l e^{j\nu_l k_1\tau}$. Therefore the radar's unambiguous time-frequency region, where it can resolve targets with no ambiguity, is $[0, \tau] \times [0, 2\pi/\tau]$ respectively. We make the following further assumptions on targets' delay and Doppler:

A4. No time ambiguity: $\{\tau_l \in I \subset [0, \tau]\}_{l=0}^{L-1}$ where I is a continuous time interval in $[0, \tau]$, so that $x_p(t) = 0, \forall t \notin [p\tau, (p+1)\tau]$.

A5. No Doppler ambiguity: $\{\nu_l \in [0, 2\pi/\tau]\}_{l=0}^{L-1}$.

A6. The pairs in the set $\{\tau_l, \nu_l\}_{l=0}^{L-1}$ are unique.

Our goal in this work is to accurately detect the L targets, i.e. to estimate the $3L$ DOF $\{\alpha_l, \tau_l, \nu_l\}_{l=0}^{L-1}$ in (2), using the least possible number of digital samples.

III. MATCHED FILTER PROCESSING

Classic radar processing samples and processes the received signal at its Nyquist rate B_h using a MF [11]. In modern systems the MF operation is performed digitally, and therefore requires an ADC capable of sampling at B_h , which can be hundreds of MHz and even up to several GHz. In order to evaluate our sampling and reconstruction method, we compare it to the classic radar processing, which in general consists of the following stages:

- 1) **ADC** – sample each incoming frame $x_p(t)$ at its Nyquist rate B_h , equal to $h(t)$'s bandwidth, creating $x_p[n], 0 \leq n < N$, where $N = \tau B_h$.

- 2) **Matched filter** – for each $x_p[n]$, create $y_p[n] = x_p[n] * h^*[-n]$, where $h[n]$ is a sampled version of the transmitted pulse $h(t)$. The time resolution attained in this step is $1/B_h$, corresponding to the width of the autocorrelation of the pulse $h(t)$.
- 3) **Doppler processing** – for each discrete time index n , perform a P -point DFT along the “slow time”: $z_n[k] = DFT_P\{y_p[n]\} = \sum_{p=0}^{P-1} y_p[n] e^{-j2\pi pk/P}$ for $0 \leq k < P$. The frequency resolution attained in this step is $2\pi/P\tau$, proportional to the inverse of the total coherent processing interval.
- 4) **Delay-Doppler map** – stacking the vectors \mathbf{z}_n , and taking absolute value, we obtain a delay-Doppler map $\mathbf{Z} = \text{abs}[\mathbf{z}_0 \dots \mathbf{z}_{N-1}] \in \mathbb{R}^{P \times N}$.
- 5) **Peak detection** – a heuristic detection process, where knowledge of number of targets, target power, clutter location, etc. may help discover target positions. For example, if we know there are L targets, then we can choose the L strongest points in the map.
- 6) **Super-resolution** – local interpolation around detected peaks helps achieve sub-pixel resolution.

Classic processing requires sampling the received signal at its Nyquist rate B_h , which is inversely proportional to the system's time resolution. The required computational power is P convolutions of a signal of length $N = \tau B_h$ and N FFTs of length P – both also proportional to B_h . The growing demands for improved estimation accuracy and target separation dictate an ever growing increase in signal's bandwidth. The goal of this work is to *break the link between radar signal bandwidth and sampling rate*, and to allow low rate sampling and processing of radar signals, regardless of their bandwidth.

We achieve this goal by utilizing the combination of ideas of FRI and Xampling. Previous works have already used these complementary concepts together. The work in [3],[9] creates a mathematical framework for sub-Nyquist sampling of pulse streams and defines lower bounds on the sampling rate needed for perfect reconstruction. Practical sampling methods achieving these bounds are explained in [2], [12], [10] in the context of ultrasound and radar, both without Doppler. Another work [7] investigates the delay-Doppler estimation problem, but assumes an infinite number of received samples and recovers the delays and Doppler frequencies in a two-stage process. We will show in Section VII that our Doppler focusing recovery method is superior to the two-stage method, where mistakes in the first stage propagate to the second stage. Combining Xampling and Doppler focusing, our $3L$ DOF input signal (2) will also enjoy the benefits of sub-Nyquist rate Xampling and accurate digital recovery of the target scene, effectively breaking the link between signal bandwidth and sampling rate.

IV. DOPPLER FOCUSING

We now introduce and explain the main idea in this paper, called Doppler Focusing. This processing technique uses target echoes from different pulses to create a single superimposed pulse, improving SNR for robustness against noise and implicitly estimating targets' Doppler frequency in the process.

We point out that stages 2) and 3) in classic processing can be viewed as delay processing and Doppler processing accordingly. Since they are both linear and time-invariant, they can be interchanged, performing the DFT before MF. In classic processing, performing MF before DFT decreases computation latency, so most practical systems carry them out in the noted order. However, when using Doppler focusing, the Doppler focusing stage must come before delay estimation and the order can no longer be reversed.

When interchanging steps 2) and 3), the DFT is simply a discrete equivalent of the following time shift and modulation operation on the received signal:

$$\begin{aligned}\Phi(t; \nu) &= \sum_{p=0}^{P-1} x_p(t + p\tau) e^{j\nu p\tau} \\ &= \sum_{p=0}^{P-1} \sum_{l=0}^{L-1} \alpha_l h(t - \tau_l) e^{j(\nu - \nu_l)p\tau} \\ &= \sum_{l=0}^{L-1} \alpha_l h(t - \tau_l) \sum_{p=0}^{P-1} e^{j(\nu - \nu_l)p\tau}\end{aligned}\quad (6)$$

where we used (4).

We now analyze the sum of exponents in (6). For any given ν , targets with Doppler frequency ν_l in a band of width $2\pi/P\tau$ around ν , i.e. in $\Phi(t; \nu)$'s “focus zone”, will achieve coherent integration and an SNR boost of approximately

$$g(\nu|\nu_l) = \sum_{p=0}^{P-1} e^{j(\nu - \nu_l)p\tau} \stackrel{|\nu - \nu_l| < 2\pi/P\tau}{\cong} P \quad (7)$$

compared with a single pulse. On the other hand, since the sum of P equally spaced points covering the unit circle is generally close to zero, targets with ν_l not “in focus” will approximately cancel out. Thus $g(\nu|\nu_l) \cong 0$ for $|\nu - \nu_l| > 2\pi/P\tau$. See Fig. 1 for an example of $g(\nu|\nu_l)$. Therefore we can approximate (6)

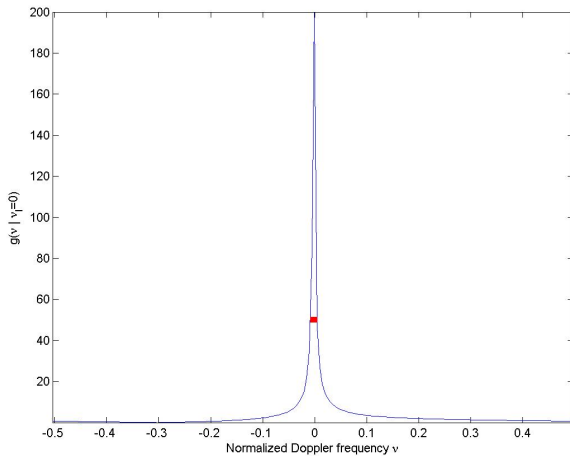


Fig. 1: Example of $g(\nu|\nu_l)$ for $P = 200$ pulses and $\nu_l = 0$. Red line marks “focus zone”, i.e. $|\nu| < 2\pi/P\tau$. Frequencies outside focus zone are severely attenuated.

by

$$\Phi(t; \nu) \cong P \sum_{l: |\nu - \nu_l| < 2\pi/P\tau} \alpha_l h(t - \tau_l). \quad (8)$$

Instead of trying to estimate delay and Doppler together, we have reduced our problem to delay only estimation for a small range of Doppler frequencies, with increased amplitude for improved performance against noise. To emphasize this, consider the case of trying to detect and estimate parameters for two targets with very closely spaced delays but with different Doppler frequencies (see for example the two helicopters in Fig. 2). Algorithms whose time resolution is coarser than the targets’ delay separation are likely to encounter various problems recovering this target scene, the most likely of which is identification of a single target instead of two. With Doppler focusing we achieve an extra dimension of potential separation, regardless of the underlying recovery algorithm, enabling improved recovery performance. Fig. 2 illustrates this concept by showing various targets spanning some delay-Doppler region. When focusing for some ν only targets in ν ’s focus zone (white region) come into view, while all other targets (red region) disappear. In Section VII we demonstrate this point via simulation.

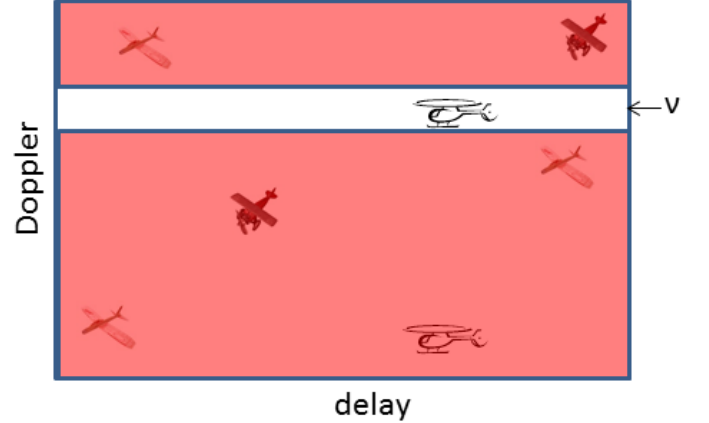


Fig. 2: Schematic delay-Doppler map. Red area indicates out-of-focus region. Only one target is in focus for current choice of ν .

To allow our sub-Nyquist recovery method, in the next sections we sample our signal in the time domain but extract frequency domain information. We now show how Doppler focusing can also be performed in the frequency domain, paving the way towards sub-Nyquist Doppler focusing.

Using (4), and denoting $X_p(\omega)$ as the CTFT of $x_p(t + p\tau)$, we have

$$X_p(\omega) = H(\omega) \sum_{l=0}^{L-1} \alpha_l e^{-j\omega\tau_l} e^{-j\nu_l p\tau}. \quad (9)$$

Taking the CTFT of $\Phi(t; \nu)$ as a function of t :

$$\begin{aligned}\Psi(\omega; \nu) &= \text{CTFT}(\Phi(t; \nu)) = \sum_{p=0}^{P-1} X_p(\omega) e^{j\nu p\tau} \\ &= H(\omega) \sum_{l=0}^{L-1} \alpha_l e^{-j\omega\tau_l} \sum_{p=0}^{P-1} e^{j(\nu - \nu_l)p\tau}.\end{aligned}\quad (10)$$

All $3L$ of the problem's parameters appear in (10). Its structure is that of a delay estimation problem as we will see in Section V, combined with the familiar sum of exponents term from (6).

We have seen that Doppler focusing reduces a delay-Doppler estimation problem to a delay-only problem for a specific Doppler frequency. In the next section we describe delay recovery from sub-Nyquist sampling rates using Xampling. In Section VI we revisit the Doppler focusing concept, combining it with these low rate Xamples to solve the delay-Doppler radar problem at sub-Nyquist rates.

V. SUB-NYQUIST DELAY RECOVERY

The problem of recovering the $2L$ amplitudes and delays in

$$\phi(t) = \sum_{l=0}^{L-1} \alpha_l h(t - \tau_l), \quad 0 \leq t < \tau \quad (11)$$

from sub-Nyquist samples has been previously studied in [2], [3], [9], [12]. Since Doppler focusing yields such a problem, we now review how Xampling can be used to solve (11) at a sub-Nyquist sampling rate.

A. Xampling

The concept of Xampling, introduced in [1], [13] and [14], describes analog-to-digital conversion which acquires samples at sub-Nyquist rates while preserving the ability to perfectly reconstruct the signal. Xampling can be interpreted as “compressed sampling”, in the sense that we are performing data compression inherently in the sampling stage. To do this, we do not simply reduce sampling rate, since this is bound to cause loss of information. Instead, we perform an analog prefiltering operation on our signal and only then sample it, in order to extract the required information for recovery. We now show how the signal's Fourier series coefficients are related to the problem's unknown parameters [3], [7], [9], [12]. We then describe how we acquire these Fourier coefficients via Xampling.

Since $\phi(t)$ is confined to the interval $t \in [0, \tau]$, it can be expressed by its Fourier series

$$\phi(t) = \sum_{k \in \mathbb{Z}} c[k] e^{j2\pi kt/\tau}, \quad t \in [0, \tau], \quad (12)$$

where

$$\begin{aligned} c[k] &= \frac{1}{\tau} \int_0^\tau \phi(t) e^{-j2\pi kt/\tau} dt \\ &= \frac{1}{\tau} \sum_{l=0}^{L-1} \alpha_l \int_0^\tau h(t - \tau_l) e^{-j2\pi kt/\tau} dt \\ &= \frac{1}{\tau} H(2\pi k/\tau) \sum_{l=0}^{L-1} \alpha_l e^{-j2\pi k\tau_l/\tau}. \end{aligned} \quad (13)$$

From (13) we see that the unknown parameters $\{\alpha_l, \tau_l\}_{l=0}^{L-1}$ are embodied in the Fourier coefficients $c[k]$ in the form of a complex sinusoid problem. For these problems, if there is no noise, $2L$ samples are enough to recover the unknown α 's and τ 's [9], i.e. $|\kappa| \geq 2L$. We can solve this problem by

using spectral analysis methods such as the annihilating filter [15] or matrix pencil [16]. One could also use MUSIC [17] or ESPRIT [18]. These recovery algorithms generally require sampling a consecutive subset of coefficients. The lower bound on $|\kappa|$ can be achieved only when the noise is negligible and computational complexity is not of concern. When there is substantial noise in the problem, having more than $2L$ coefficients will allow the recovery to be more robust.

Our signals exist in the time domain, and therefore we do not have direct access to $c[k]$. We can use the Direct Multichannel Sampling scheme described in [3] in order to obtain the Fourier series coefficients. Fig. 3 demonstrates a Xampling scheme used to directly extract the required Fourier coefficients from the signal. In [2] an actual radar system was built using a similar yet more practical technique, where a set of mixers, band-pass filters and low rate ADCs sampled different spectral bands of the signal and the matching Fourier coefficients were created digitally. The radar model there included delay only without Doppler. An alternative Xampling method uses the Sum of Sincs filter as described in [12]. All of these methods can be used to obtain arbitrary Fourier series coefficients. The number of Fourier coefficients extracted per pulse is a design parameter which controls the tradeoff between sampling rate and recovery performance. In our numerical experiments, presented in Section VII, we demonstrate a Xampling rate one tenth of the Nyquist rate.

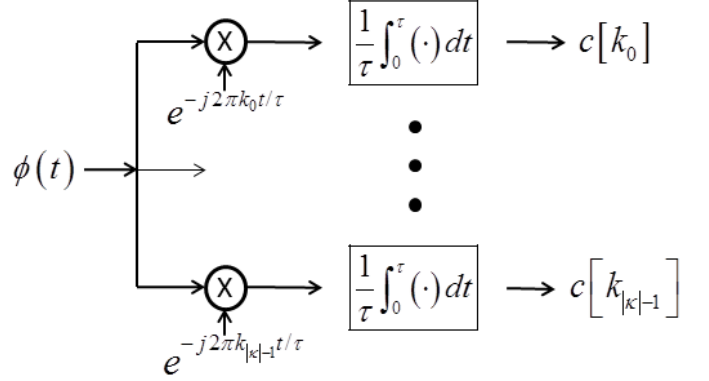


Fig. 3: Multichannel direct sampling of the Fourier series coefficients, from [3].

B. Compressed Sensing Recovery

In the previous subsection we showed that $2L$ samples are enough to solve (11), when there is no noise. We now describe a CS-based recovery method, operating on the Xamples $c[k]$, which is more robust to noise.

Assume the time delays are aligned to a grid

$$\tau_l = q_l \Delta_\tau, \quad 0 \leq q_l < N_\tau \quad (14)$$

where we choose Δ_τ so that $N_\tau = \tau/\Delta_\tau$ is an integer. Choose a set of indices $\kappa = \{k_0, \dots, k_{|\kappa|-1}\}$, and define the corresponding vector of Fourier coefficients

$$\mathbf{c} = [c[k_0] \dots c[k_{|\kappa|-1}]]^T \in \mathbb{C}^{|\kappa|}. \quad (15)$$

We can then write (13) in vector form as

$$\mathbf{c} = \frac{1}{\tau} \mathbf{H} \mathbf{V} \mathbf{x} \quad (16)$$

where \mathbf{H} is a $|\kappa| \times |\kappa|$ diagonal matrix with diagonal elements $H(2\pi k_i/\tau)$ and \mathbf{V} is a $|\kappa| \times N_\tau$ matrix with elements $\mathbf{V}_{mq} = e^{-j2\pi k_m q/N_\tau}$, i.e. it is composed of $|\kappa|$ rows of the $N_\tau \times N_\tau$ DFT matrix. The vector $\mathbf{x} \in \mathbb{C}^{N_\tau}$ is L -sparse, where each index q contains the amplitude of a target with delay $q\Delta_\tau$ if it exists, or zero otherwise. Defining the CS dictionary $\mathbf{A} = \frac{1}{\tau} \mathbf{H} \mathbf{V} \in \mathbb{C}^{|\kappa| \times N_\tau}$ we obtain the CS equation

$$\mathbf{c} = \mathbf{A} \mathbf{x}. \quad (17)$$

Estimating targets' delays can be carried out by solving (17) and finding \mathbf{x} 's support - any nonzero index q denotes a target with delay $q\Delta_\tau$.

For any set of sampled Fourier coefficients, a variety of CS techniques can be employed for recovery [10], for instance orthogonal matching pursuit (OMP) [19], iterative hard thresholding (IHT) [20], or L1 minimization ([21] and references within). Also, choosing the coefficients at random produces favorable conditions for CS, aiding recovery in the presence of noise. If the indices in κ are selected uniformly at random, it can be shown that if $|\kappa| \geq CL(\log N_\tau)^4$, for some positive constant C , then \mathbf{A} obeys the desired Restricted Isometry Property (RIP) with large probability [22]. By satisfying the condition for RIP we are able to recover \mathbf{x} , using a CS recovery algorithm.

VI. DELAY-DOPPLER RECOVERY USING DOPPLER FOCUSING

In Section IV we introduced the concept of Doppler focusing, and in Section V we reviewed how to Xample and recover the $2L$ unknowns of the delay-only problem (11). We now return to our original delay-Doppler problem (2).

We begin by describing how the target scene can be recovered perfectly when there is no noise, at a sample rate proportional to the signal's rate of innovation. This recovery method is not robust to noise, motivating the use of Doppler focusing, described after we show how Xampling can be performed on the multi-pulse signal (2). Finally we discuss some practical considerations and compare our method to previous CS approaches.

A. Noiseless Recovery

We are interested in analyzing the noiseless scenario in order to find the minimal number of samples K_{min} needed for perfect recovery of our problem's $3L$ unknown parameters. Since K_{min} cannot be smaller than the number of DOF, $K_{min} \geq 3L$. We now describe a reconstruction method capable of perfectly estimating all $3L$ unknowns using $4L$ samples, slightly above the minimal rate but still significantly below the Nyquist rate for reasonable B_h and L .

Defining $\beta_l^p = \alpha_l e^{-j\nu_l p\tau}$ we obtain

$$c_p[k] = \frac{1}{\tau} H(2\pi k/\tau) \sum_{l=0}^{L-1} \beta_l^p e^{-j2\pi k \tau_l/\tau}. \quad (18)$$

Choosing a set of indices k for which $H(2\pi k/\tau) \neq 0$, we can preprocess the coefficients $c_p[k]$ by the inverse $H^{-1}(2\pi k/\tau)$ to obtain a standard spectral analysis problem, as we have seen in Section V. For these problems, $2L$ samples are enough to perfectly recover the unknown β 's and τ 's, if there is no noise.

Suppose we have used $2L$ samples to solve (18) for some $0 \leq p \leq P-2$. We now possess the set of delays $\{\tau_l\}_{l=0}^{L-1}$, thus recovering the first L DOF. We also possess the set $\{\beta_l^p\}_{l=0}^{L-1}$, to be used shortly. To recover the remaining $2L$ DOF, we solve (18) for $p' = p+1$, obtaining $\{\beta_l^{p'}\}_{l=0}^{L-1}$. Since

$$\beta_l^{p'} = \alpha_l e^{-j\nu_l p'\tau} = \alpha_l e^{-j\nu_l (p+1)\tau} = \beta_l^p e^{-j\nu_l \tau}, \quad (19)$$

we can recover the set of Doppler frequencies by

$$\nu_l = \frac{1}{\tau} \angle \left(\frac{\beta_l^p}{\beta_l^{p'}} \right). \quad (20)$$

Using (20), recovery of the set of amplitudes is immediate from $\alpha_l = \beta_l^p e^{j\nu_l p\tau}$.

To conclude, we have shown a reconstruction method for the noiseless scenario, which perfectly recovers the problem's $3L$ unknown parameters using only $4L$ samples. In order to provide robustness to noise, we now combine Xampling with Doppler focusing.

B. Xampling

Similarly to the Xampling technique of Section V which obtained $c[k]$, we can extend this technique to each of the pulses $x_p(t)$ of the multi-pulse signal (2) to obtain $c_p[k]$. Since $x_p(t)$ is confined to the interval $t \in [p\tau, (p+1)\tau]$, we can replace $t \rightarrow t + p\tau$ and $\alpha_l \rightarrow \alpha_l e^{-j\nu_l p\tau}$ in (13) to obtain

$$c_p[k] = \frac{1}{\tau} H(2\pi k/\tau) \sum_{l=0}^{L-1} \alpha_l e^{-j\nu_l p\tau} e^{-j2\pi k \tau_l/\tau}, \quad (21)$$

where we used the fact that since both $k, p \in \mathbb{Z}$ we have $e^{-j2\pi kp} \equiv 1$. From (21) we see that all $3L$ unknown parameters $\{\alpha_l, \tau_l, \nu_l\}_{l=0}^{L-1}$ are embodied in the Fourier coefficients $c_p[k]$ in the form of a complex sinusoid problem.

C. Applying Doppler Focusing and CS Recovery

Having acquired $c_p[k]$ using Xampling, we now perform the Doppler focusing operation for a specific frequency ν

$$\begin{aligned} \Psi_\nu[k] &= \sum_{p=0}^{P-1} c_p[k] e^{j\nu p\tau} \\ &= \frac{1}{\tau} H(2\pi k/\tau) \sum_{l=0}^{L-1} \alpha_l e^{-j2\pi k \tau_l/\tau} \sum_{p=0}^{P-1} e^{j(\nu - \nu_l)p\tau}. \end{aligned} \quad (22)$$

From (10) we see that $\Psi_\nu[k] = \Psi(\omega; \nu)|_{\omega=2\pi k/\tau}$.

Following the same arguments as in (7), for any target l satisfying $|\nu - \nu_l| < 2\pi/P\tau$ we have

$$\sum_{p=0}^{P-1} e^{j(\nu - \nu_l)p\tau} \cong P. \quad (23)$$

Therefore, Doppler focusing can be performed on the low rate sub-Nyquist samples:

$$\Psi_\nu[k] \cong \frac{P}{\tau} H(2\pi k/\tau) \sum_{l: |\nu - \nu_l| < 2\pi/P\tau} \alpha_l e^{-j2\pi k\tau_l/\tau}. \quad (24)$$

Equation (24) is identical in form to (13) except it is scaled by P , increasing SNR for improved performance with noise. Furthermore, we reduced the number of active delays. For each ν we now have a delay estimation problem, which can be written in vector form using the same notations of Section V as

$$\Psi_\nu = \frac{P}{\tau} \mathbf{H} \mathbf{V} \mathbf{x}_\nu \quad (25)$$

where

$$\Psi_\nu = [\Psi_\nu[k_0] \dots \Psi_\nu[k_{|\kappa|-1}]]^T \in \mathbb{C}^{|\kappa|}. \quad (26)$$

This is exactly the CS problem we have already shown how to solve, with one important difference. In the delay-only problem of Section V, the model order L was known. Here, since there are L targets but we have no prior knowledge of their distribution in the delay-Doppler grid, for each ν we must either estimate the model order $0 \leq L_\nu \leq L$, or take a worst case approach and assume $L_\nu = L$. The problem of estimating the number of sinusoids in a noisy sequence has been studied extensively [23], [24], [25]. Solving (25) with an accurate model order can decrease computation time (although estimating model order is also time consuming) and possibly reduce detection of spurious targets. The former option is preferable in higher SNR scenarios when the L_ν estimates are good, while the latter can be a fall back approach in noisy scenarios when the L_ν estimates contain significant error. In our simulations, since we do not want model order errors to influence recovery performance, we employ the worst case approach.

The Doppler focusing technique is a continuous operation on the variable ν , and can be performed for any Doppler frequency up to the PRF. Since the focus zone for each ν is of width $2\pi/P\tau$, we can find various finite sets of ν 's spanning $[0, 2\pi/\tau]$. For any such set, define its size as N_ν . For each ν in the set, we solve (25) assuming \mathbf{x}_ν 's support is of size L . This problem can be solved using an abundance of CS algorithms as described in Section V. After solving N_ν separate CS problems with dictionary of size $|\kappa| \times N_\tau$, we hold at most LN_ν estimated amplitudes. Since the absolute value of amplitudes recovered in the support is indicative of true target existence as opposed to noise, we sort the LN_ν estimated amplitudes according to their absolute value, and take the L strongest ones as true target locations. Algorithm 1 summarizes the Doppler focusing algorithm.

D. Practical Considerations

If the set of probed Doppler frequencies lies on a uniform grid, i.e. $\nu_n = 2\pi n/N_\nu\tau$, $n = 0, 1, \dots, N_\nu - 1$, then $\Psi_\nu[k]$ can be created efficiently using a length N_ν DFT or FFT of a

Algorithm 1 Doppler Focusing

Input: Samples $\{c_p[k]\}_{0 \leq p < P}^{k \in \kappa}$

Output: Estimated target parameters $\{\hat{\alpha}_l, \hat{\tau}_l, \hat{\nu}_l\}_{l=0}^{L-1}$

Initialization: Discretize unambiguous Doppler interval $[0, 2\pi/\tau]$ into N_ν points $\{\nu_n\}_{n=0}^{N_\nu-1}$, where the union of focus zones of all points covers the interval.

for $n = 0$ to $N_\nu - 1$ **do**

Create Ψ_{ν_n} from $\{c_p[k]\}_{0 \leq p < P}^{k \in \kappa}$ using Doppler focusing (22)

Solve $\Psi_{\nu_n} = \frac{P}{\tau} \mathbf{H} \mathbf{V} \mathbf{x}_n$ for \mathbf{x}_n to obtain $\{\hat{\alpha}_l^n, \hat{\tau}_l^n\}_{l=0}^{L-1}$

end for

Sort $\{\{\hat{\alpha}_l^n\}_{0 \leq l < L}^{0 \leq n < N_\nu}\}$, denoting indices of L largest values as $\{l_i, n_i\}_{i=0}^{L-1}$.

for $i = 0$ to $L - 1$ **do**

$\hat{\alpha}_i \leftarrow \hat{\alpha}_{l_i}^{n_i}; \quad \hat{\tau}_i \leftarrow \hat{\tau}_{l_i}^{n_i}; \quad \hat{\nu}_i \leftarrow \nu_{n_i}$

end for

series of length P :

$$\begin{aligned} \Psi_n[k] &\triangleq \Psi_{\nu_n}[k] = \sum_{p=0}^{P-1} c_p[k] e^{j\nu_n p\tau} \\ &= \sum_{p=0}^{P-1} c_p[k] e^{j2\pi n p/N_\nu} = DFT_{N_\nu}\{c_p[k]\}. \end{aligned} \quad (27)$$

When focusing on some Doppler frequency ν , targets with Doppler frequencies ν_l satisfying $|\nu_l - \nu| > 2\pi/P\tau$ are considered undesirable and we seek to minimize their effect. These targets can be viewed as “out-of-focus”, since they are not matched to ν and their responses from different pulses do not combine coherently; they will combine in phase for different ν 's satisfying $|\nu_l - \nu| < 2\pi/P\tau$. We can add to (22) a user defined weighting function $w[p]$, $p = 0, 1, \dots, P - 1$ (e.g. Hann, Blackman, etc.) which is designed to mitigate the impact of these out-of-focus targets:

$$\begin{aligned} \Psi_\nu[k] &= \sum_{p=0}^{P-1} c_p[k] e^{j\nu p\tau} w[p] \\ &= \frac{1}{\tau} H(2\pi k/\tau) \sum_{l=0}^{L-1} \alpha_l e^{-j2\pi k\tau_l/\tau} \sum_{p=0}^{P-1} e^{j(\nu - \nu_l)p\tau} w[p]. \end{aligned} \quad (28)$$

The drawback of weighting is that it increases the frequency's focus zone, potentially including more targets in each delay estimation problem. In Fig. 4 we see an example of how weighting functions can reduce the effect of out-of-focus targets compared with no weighting (constant $w[p]$). For a comprehensive review of weighting function design considerations see [26].

Slow time undersampling, i.e. sampling only a subset of the P transmitted pulses, is a natural extension of the Doppler focusing method. Instead of Xampling all P pulses to obtain $c_p[k]$ for $p = 0, 1, \dots, P - 1$, and then combining them all as in (22), we can work with a subset of the pulses $\Gamma \subset \{0, 1, \dots, P - 1\}$. Undersampling using Γ is advantageous in the same ways as fast time undersampling: reducing hardware,

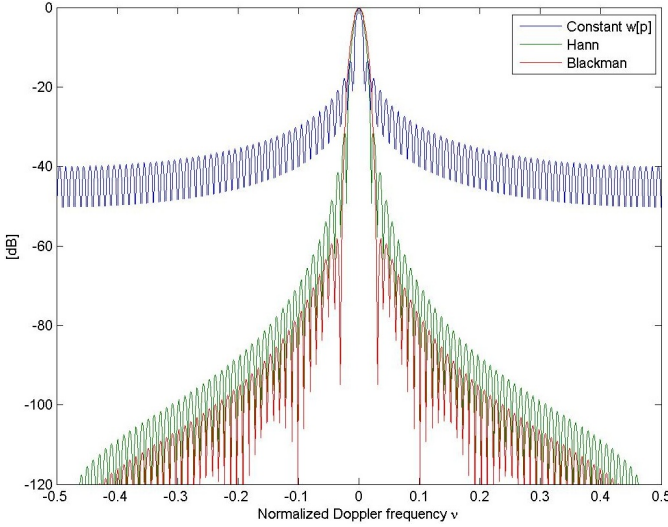


Fig. 4: DFT of weighting functions $w[p]$ compared with no weighting (constant $w[p]$) for $P = 100$ pulses. Attenuation of targets with Doppler frequencies far enough from nominal frequency ($\nu = 0$ in this case) increases significantly with proper weighting. Also, focus zone changes for different $w[p]$'s.

processing and storage requirements. The disadvantage of slow time undersampling is also like that of fast time - a decrease in SNR and possible decline in estimation performance. It adds another degree of freedom to the sampling and recovery architecture, allowing to split the undersampling ratio between fast and slow time samples and balancing the tradeoff between them. For example, a system with storage constraints, may use Γ to dilute the number of processed pulses while maintaining a higher fast time sample rate.

E. Previous CS Approaches

A possible approach to the problem at hand could be a two-stage CS recovery technique, first estimating target delays and afterwards for each delay estimating Doppler frequency (or vice versa). These two-stage methods tend to be suboptimal since the problem is not separable, and a mistake in the first estimation stage propagates to the second stage where it cannot be undone. We compare our method to this type of recovery in Section VII.

To overcome this inefficiency, several works [5], [8] employ a single stage CS recovery technique. Instead of estimating delays and Doppler frequencies separately and sequentially, they estimate the most likely (τ_l, ν_l) pairs. The drawback of this technique is that it requires using a dictionary with dimensions proportional to $N_\tau N_\nu F_s$, where F_s is the problem's sample rate. Since grid sizes can easily reach 10^3 , and sample rates are on the order of MHz, the dictionary grows rapidly rendering these methods infeasible for even moderate problem size.

VII. SIMULATION RESULTS

In the previous sections we described the Doppler focusing approach to delay-Doppler recovery. Before showing

numerical examples comparing our method to other recovery techniques, we first discuss how the user defined performance metric influences grid size and Fourier coefficient selection.

A. Performance Metric

Our problem lies in a continuous, analog world. Since we choose to solve it using CS, which is an approach developed for discrete problems, we must discretize the delay grid, to steps of size Δ_τ . As real world targets delays and Doppler frequencies do not lie on any predefined grid, but our CS recovery assumes they do, it seems we should take $\Delta_\tau \rightarrow 0$ in order to minimize discretization errors. Computational requirements aside, there is one significant drawback to such a decrease in grid step - columns in the CS dictionary \mathbf{A} become increasingly similar, making \mathbf{A} increasingly coherent, where coherence is defined as the largest absolute inner product between any two columns $\mathbf{a}_i, \mathbf{a}_j$ of \mathbf{A} :

$$\mu(\mathbf{A}) = \max_{i \neq j} \frac{|\langle \mathbf{a}_i, \mathbf{a}_j \rangle|}{\|\mathbf{a}_i\|_2 \|\mathbf{a}_j\|_2}. \quad (29)$$

A basic premise of CS ties low coherence to successful recovery [27]. Therefore, \mathbf{A} is usually designed to have small coherence. This contradicts taking the step size to be very small.

Here, we move away from this basic assumption, and argue that depending on the chosen performance metric, high coherence can actually help recovery instead of harm it. For example, assume we are interested in delay recovery but are tolerant of some small error τ_{max} . In radar applications, a common performance metric is the “hit-or-miss” criterion on the estimated delays $\{\hat{\tau}_l\}_{l=0}^{L-1}$:

$$e_l(\hat{\tau}_l) = \begin{cases} 0, & \text{if } |\tau_l - \hat{\tau}_l| < \tau_{max} \\ 1, & \text{otherwise} \end{cases} \quad (30)$$

$$e = \sum_{l=0}^{L-1} e_l.$$

Translating τ_{max} to a condition on support recovery, (30) tolerates an error of no more than $K = \lfloor \tau_{max} / \Delta_\tau \rfloor \in \mathbb{N}$ places in the recovered indices from (17), where we assume $K \geq 1$. Instead of designing \mathbf{A} so that each column is as non-correlative with the other columns as possible, we can try to design the dictionary so that each column is somewhat correlative with its K nearest neighbours, and only afterwards does the correlation drop. This will improve recovery performance in noisy scenarios since in cases where the correct column is not recovered, any one of its similar neighbouring columns still has a chance to overcome the noise and produce a “hit”. Graphs in the next subsection will show how such a coherent \mathbf{A} actually improves recovery performance compared with a less coherent dictionary in very noisy scenarios.

If τ_{max} is chosen so that $K = 0$, the same line of thought entails requiring each dictionary column to be similar to 0 neighbours, i.e. for \mathbf{A} to have minimal coherence. Since most CS works deal with exact recovery, this explains why they strive for a minimal $\mu(\mathbf{A})$.

We can control the level of \mathbf{A} 's coherence by choosing different sets of Fourier coefficient κ in (15). Fig. 5 shows

an example of the column correlation pattern for two sets of Fourier coefficients: a consecutive set and a random set, where all coefficients were chosen in $[-B_h/2, B_h/2]$. We define the column correlation function for some column \mathbf{a}_i as

$$\mu_i[j] = \frac{|\langle \mathbf{a}_i, \mathbf{a}_j \rangle|}{\|\mathbf{a}_i\|_2 \|\mathbf{a}_j\|_2}. \quad (31)$$

The consecutive set is better suited for performance criteria which allow some error in support recovery, while the random set will achieve better performance when exact recovery is required.

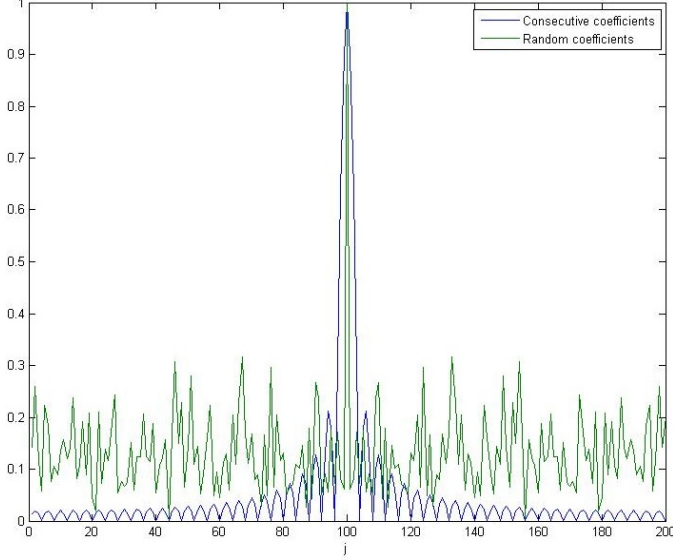


Fig. 5: Column correlation pattern $\mu_0[j]$ of the CS dictionary from (17) for two sets κ . The consecutive set achieves coherence of 0.9 due to the many correlative columns in the center, while the random set has coherence of 0.3.

B. Numerical Results

We now present some numerical experiments illustrating the recovery performance of a sparse target scene. We corrupt the received signal $x(t)$ with an additive white Gaussian noise $n(t)$ with power spectral density $S_n(f) = N_0/2$, bandlimited to $x(t)$'s bandwidth B_h . We define the signal to noise power ratio for target l as

$$\text{SNR}_l = \frac{\frac{1}{T_p} \int_0^{T_p} |\alpha_l h(t)|^2 dt}{N_0 B_h}, \quad (32)$$

where T_p is the pulse time. The scenario parameters used were number of targets $L=5$, number of pulses $P=100$, PRI $\tau=10\mu\text{sec}$, and $B_h=200\text{MHz}$. The classic time and frequency resolutions ("Nyquist bins"), defined as $1/B_h$ and $1/P\tau$, are 5nsec and 1kHz accordingly. In order to demonstrate a 1:10 sampling rate reduction, our sub-Nyquist Xampling scheme generated 200 Fourier coefficients per pulse, as opposed to the 2000 Nyquist rate samples. We tested Doppler focusing with two types of Fourier coefficient sets κ , a consecutive set and a random set. We compared Doppler focusing recovery performance with classic processing and a two-stage recovery

method as described in [7] (where we use a CS algorithm instead of ESPRIT) using the following criteria:

- 1) **Hit-Rate** – we define a "hit" as a delay-Doppler estimate which is circumscribed by an ellipse around the true target position in the time-frequency plane. We used an ellipse with axes equivalent to ± 3 times the time and frequency Nyquist bins.
- 2) **Recovery RMS error** – for estimates classified as hits, we measure the root mean square error in both time and frequency.

As noted in the previous section, a single stage CS recovery method using Nyquist bins spacing consumes a prohibitive amount of memory and was not able to run on any computer at hand, since the CS dictionary required storing $4 \cdot 10^9$ elements (occupying 32GB of memory using standard IEEE double precision): $\frac{2\pi/\tau}{2\pi/P\tau} \frac{\tau}{1/B_h} = P\tau B_h = 2 \cdot 10^5$ columns and $P\tau B_h/10 = 2 \cdot 10^4$ measurements per column.

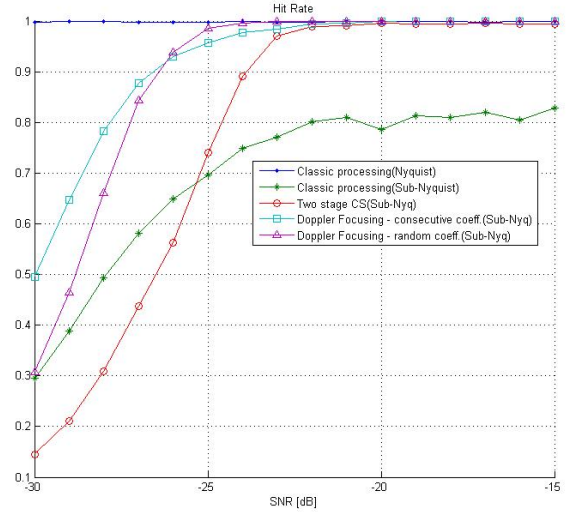


Fig. 6: Hit Rate for classic processing, two-stage CS recovery and Doppler focusing as function of SNR. Sub-Nyquist sampling rate was one tenth the Nyquist rate.

For CS-based techniques, the delay grid step Δ_τ was chosen as half a Nyquist bin. For Doppler focusing, the Doppler frequency region was discretized with uniform steps of half a Nyquist bin. To provide a fair comparison, classic processing performed the slow time FFT after padding with P zeros.

Fig. 6 and Fig. 7 demonstrate the hit-rate and RMS error performance of the different recovery methods for various SNR values. It is evident that Doppler focusing is superior to the other sub-Nyquist recovery techniques. Between the two Doppler focusing approaches, consecutive coefficients are better suited for lower SNR, while choosing coefficients randomly improves performance as SNR increases. Since both sets κ produce CS dictionaries with column correlation functions which are not matched to the "hit-or-miss" performance criteria used, we have no reason to assume one should be better than the other. Also, random coefficients, when producing a hit, have very small delay errors (even compared with Nyquist rate classic processing) due to low CS dictionary coherence.

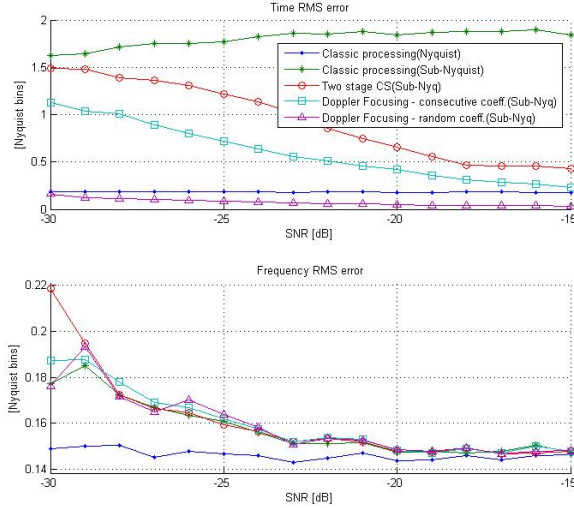


Fig. 7: RMS error of time and frequency estimates for classic processing, two-stage CS recovery and Doppler focusing as function of SNR. Sub-Nyquist sampling rate was one tenth the Nyquist rate.

Fig. 8 shows the sparse target scene on a time-frequency map for a -28dB SNR scenario, where each target is displayed along with its hit rate ellipse, together with the various sub-Nyquist recovery methods' estimates and hit rates. As noted in Section IV, only Doppler focusing is able to distinguish between the two targets having almost identical delays (around $4.2 \mu\text{sec}$) but different Doppler frequencies.

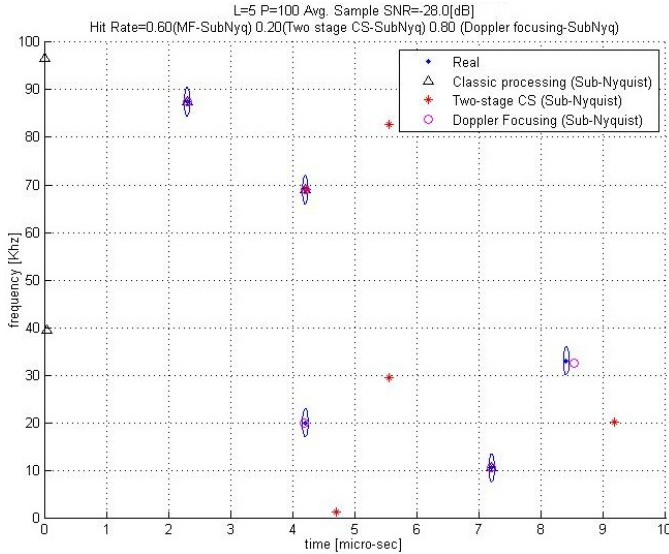


Fig. 8: Real target positions along with various estimates. Doppler focusing achieves highest hit rate among sub-Nyquist methods. Only Doppler focusing detects two targets around $4.2 \mu\text{sec}$.

VIII. CONCLUSION

We demonstrated a radar sampling and recovery method called Doppler focusing, which employs the techniques of

Xampling and CS, and is independent of the radar signal's bandwidth. Doppler focusing allows for low rate sampling and digital processing and undersampling in both fast and slow time. It also leads to CS recovery with dictionary size scaling with delay grid size only, and imposes no constraints on transmitted signal or modulation. We compared our method to other sub-Nyquist recovery techniques and have seen its clear advantage in simulations. When sampling at one tenth the Nyquist rate, and for SNR above -25dB, Doppler focusing achieves results almost identical to classic recovery working at the Nyquist rate.

APPENDIX

In the following section we formally define assumptions **A1-A3**. For this we define a few auxiliary parameters that were previously unneeded. Denote the radar's carrier frequency as f_c , the pulse time support as T_p , and the speed of light as c . We use the time-distance equivalence $r_l = c\tau_l/2$ and the non-relativistic Doppler radial frequency-velocity equivalence $\dot{r}_l = \nu_l c/4\pi f_c$.

A1. "Far targets" - target-radar distance is large compared to the distance change during observation interval

$$\begin{aligned} \dot{r}_l P\tau &\ll r_l \\ \nu_l c P\tau / 4\pi f_c &\ll c\tau_l / 2 \\ \nu_l &\ll 2\pi f_c \tau_l / P\tau. \end{aligned} \quad (33)$$

A2. "Slow targets" - we can assume constant τ_l if the base-band Doppler frequency is smaller than the frequency resolution

$$\begin{aligned} 2\dot{r}_l B_h / c &\ll 1/P\tau \\ \nu_l B_h / 2\pi f_c &\ll 1/P\tau \\ \nu_l &\ll 2\pi f_c / P\tau B_h. \end{aligned} \quad (34)$$

This inequality is termed the "narrowband assumption" in radar nomenclature, since it gives an upper limit on the radar signal's bandwidth.

We can assume the Doppler induced phase change over a single pulse time is small if $\nu_l T_p \ll 1$.

A3. "Small acceleration" - velocity change induced by acceleration is smaller than velocity resolution

$$\begin{aligned} \ddot{r}_l P\tau &\ll c/2f_c P\tau \\ \ddot{r}_l &\ll c/2f_c (P\tau)^2. \end{aligned} \quad (35)$$

REFERENCES

- [1] M. Mishali, Y. C. Eldar, O. Dounaevsky, and E. Shoshan, "Xampling: Analog to Digital at Sub-Nyquist Rates," *IET Circuits, Devices and Systems*, vol. 5, no. 1, pp. 8–20, Jan. 2011.
- [2] E. Baransky, G. Itzhak, I. Shmuel, N. Wagner, E. Shoshan, and Y. C. Eldar, "A Sub-Nyquist Radar Prototype: Hardware and Algorithms," submitted to *IEEE Transactions on Aerospace and Electronic Systems, special issue on Compressed Sensing for Radar*, Aug. 2012.
- [3] K. Gedalyahu, R. Tur, and Y. C. Eldar, "Multichannel Sampling of Pulse Streams at the Rate of Innovation," *IEEE Transactions on Signal Processing*, vol. 59, no. 4, pp. 1491–1504, Apr. 2011.
- [4] M. A. Herman and T. Strohmer, "High-Resolution Radar via Compressed Sensing," *Transactions on Signal Processing*, vol. 57, no. 6, pp. 2275–2284, Jun. 2009.

- [5] B. Demissie, "High-Resolution Range-Doppler Imaging by Coherent Block-Sparse Estimation," *International Workshop on Compressed Sensing Applied to Radar*, May 2012.
- [6] R. G. Baraniuk and P. Steeghs, "Compressive Radar Imaging," in *IEEE Radar Conference*, Waltham, MA, Apr. 2007.
- [7] W. U. Bajwa, K. Gedalyahu, and Y. C. Eldar, "Identification of Parametric Underspread Linear Systems and Super-Resolution Radar," *IEEE Transactions on Signal Processing*, vol. 59, no. 6, pp. 2548–2561, June 2011.
- [8] J. Zhang, D. Zhu, and G. Zhang, "Adaptive Compressed Sensing Radar Oriented Toward Cognitive Detection in Dynamic Sparse Target Scene," *IEEE Transactions on Signal Processing*, vol. 60, no. 4, pp. 1718–1729, Apr. 2012.
- [9] M. Vetterli, P. Marziliano, and T. Blu, "Sampling Signals with Finite Rate of Innovation," *IEEE Transactions on Signal Processing*, vol. 50, no. 6, pp. 1417–1428, 2002.
- [10] N. Wagner, Y. C. Eldar, and Z. Friedman, "Compressed Beamforming in Ultrasound Imaging," *IEEE Transactions on Signal Processing*, vol. 60, no. 9, pp. 4643–4657, Sep. 2012.
- [11] M. Skolnik, *Radar Handbook*. McGraw Hill, New York, NY, USA, 1970.
- [12] R. Tur, Y. C. Eldar, and Z. Friedman, "Innovation Rate Sampling of Pulse Streams with Application to Ultrasound Imaging," *IEEE Transactions on Signal Processing*, vol. 59, no. 4, pp. 1827–1842, Apr. 2011.
- [13] M. Mishali and Y. C. Eldar, *Xampling: Compressed Sensing for Analog Signals*, Y. C. Eldar and G. Kutyniok, Eds. Cambridge University Press, 2012.
- [14] M. Mishali, Y. C. Eldar, and A. Elron, "Xampling: Signal Acquisition and Processing in Union of Subspaces," *IEEE Transactions on Signal Processing*, vol. 59, no. 10, pp. 4719–4734, Oct. 2011.
- [15] P. Stoica and R. Moses, *Introduction to Spectral Analysis*. Englewood Cliffs, NJ: Prentice-Hall, 2000.
- [16] T. K. Sarkar and O. Pereira, "Using the Matrix Pencil Method to Estimate the Parameters of a Sum of Complex Exponentials," *IEEE Antennas and Propagation Magazine*, vol. 37, no. 1, pp. 48–55, Feb. 1995.
- [17] R. Schmidt, "Multiple Emitter Location and Signal Parameter Estimation," *IEEE Transactions on Antennas Propagation*, vol. 34, no. 3, pp. 276–280, Mar. 1986.
- [18] R. Roy and T. Kailath, "ESPRIT-Estimation of Signal Parameters via Rotational Invariance Techniques," *IEEE Transactions on Acoustics, Speech and Signal Processing*, vol. 37, no. 7, pp. 984–995, Jul. 1989.
- [19] S. G. Mallat and Z. Zhang, "Matching Pursuits with Time-Frequency Dictionaries," *IEEE Transactions on Signal Processing*, vol. 41, no. 12, pp. 3397–3415, Dec. 1993.
- [20] T. Blumensath and M. Davies, "Iterative Hard Thresholding for Compressive Sensing," *Applied Computational Harmonic Analysis*, vol. 27, no. 3, pp. 265–274, 2009.
- [21] Y. C. Eldar and G. Kutyniok, Eds., *Compressed Sensing: Theory and Applications*. Cambridge University Press, May 2012.
- [22] M. Rudelson and R. Vershynin, "On Sparse Reconstruction from Fourier and Gaussian Measurements," *Communications on Pure and Applied Mathematics*, vol. 61, no. 8, pp. 1025–1045, 2008.
- [23] G. Schwartz, "Estimating the Dimension of a Model," *Annals of Statistics*, vol. 6, no. 2, pp. 461–464, 1978.
- [24] M. Wax and T. Kailath, "Detection of Signals by Information Theoretic Criteria," *IEEE Transactions on Acoustics, Speech and Signal Processing*, vol. 33, no. 2, pp. 387–392, Apr. 1985.
- [25] J. J. Fuchs, "Estimating the Number of Sinusoids in Additive White Noise," *IEEE Transactions on Acoustics, Speech and Signal Processing*, vol. 36, no. 12, pp. 1846–1853, Dec. 1988.
- [26] F. J. Harris, "On the use of Windows for Harmonic Analysis with the Discrete Fourier Transform," *Proceedings of the IEEE*, vol. 66, no. 1, pp. 51–83, Jan. 1978.
- [27] M. F. Duarte and Y. C. Eldar, "Structured Compressed Sensing: From Theory to Applications," *IEEE Transactions on Signal Processing*, vol. 59, pp. 4053–4085, Sep. 2011.